Spatio-Temporal Analysis of Abrasion Susceptibility Effect on Land Cover in the Coastal Area of Bantul Regency, Yogyakarta, Indonesia

Pratama, D. N. D.,[1] Khakhim, N.,[1] Wicaksono, A.,[1,2] Musthofa, A.[3] and Lazuardi, W.[1,2].
[1]Department of Geographic Information Science, Faculty of Geography, Universitas Gadjah Mada, Yogyakarta, Indonesia
[2]The Master Program in Planning and Management of Coastal and Watershed, Faculty of Geography, Universitas Gadjah Mada, Yogyakarta, Indonesia
[3]Department of Development Geography, Faculty of Geography, Universitas Gadjah Mada, Yogyakarta, Indonesia
E-mail: nurulk@ugm.ac.id
DOI: https://doi.org/10.52939/ijg.v17i4.1961

Abstract
Shoreline dynamics naturally occur in coastal areas, and over time, are also influenced by anthropogenic processes taking place both on-site and upstream. Bordering the Indian Ocean, the coastal area of Bantul Regency in the Special Region of Yogyakarta is faced with typical strong and high waves that induce changes in its shoreline dynamics and activities. Consequently, tourism, a leading economic sector in the area, often needs to adjust to such changes. Here, shorelines were extracted from the spatial data of time-series Sentinel 2A imagery (2015, 2016, 2017, 2018, 2019, and 2020) using water index transformation, MNDWI, while the land cover changes were analyzed using the Decision Tree classification. Based on the results, accretion appeared most significant from 2016 to 2017, creating an additional 22.32 ha. In contrast, shoreline change from 2019 until 2020 indicated the most severe abrasion that led to a loss of 34.89 ha. The highest rate of landward shoreline change was 41.58 m/year.

1. Introduction

Indonesia consists of around 16,671 named islands (UNGEGN, 2019) scattered throughout its territorial waters, making it one of the world's largest archipelagic countries. Also, for this reason, it has the fourth-longest shoreline worldwide, which exceeds 95,000 km (Rais et al., 2004). In 2018, Indonesia Coordinating Minister for Maritime Affairs and Investment claimed that the country had a 108,000 km long shoreline.

Shorelines create a boundary between land and sea with position moving from time to time and a zone where sea-level fluctuations caused by, for example, tides are perceptible (CERC, 1984). They are a dynamic object that marks changes between land and sea and is heavily influenced by waves, winds, nearshore currents, and human activities. It is estimated that there are more than 35,984 shorelines globally, and 60% of the world's population establishes their activities about 100 km from the sea (Vitousek et al., 1997). Shorelines shift in either quick or slow succession depending on the sediment equilibrium between nearshore sediment motion by waves and currents (Triatmodjo, 2008), topography (Sinaga and Susiati, 2007), coastal material, tides, and wind (Dulbahri, 1983). Seasons can significantly influence the position of shoreline, such as the tide that occurs and the wave conditions when the shoreline is mapped (Moore, 2000).

The dynamics of shoreline changes shape abrasion susceptibility in coastal areas. Shoreline changes can impact land cover in coastal areas and vice versa. Land cover is a physical appearance of activities on it. In coastal regions, activities can form shoreline dynamics and, at the same time, be affected by abrasion susceptibility in coastal areas. The coastal area in Bantul Regency lies on the southern coast of Java Island and directly faces the Indian Ocean. Here, human activities are carried out massively, including tourism that has been one of the leading sectors capable of bringing in tourists from other cities and contributing to regional income. The effect of abrasion susceptibility on land cover in this coastal area needs to be spatiotemporally studied to determine the dynamics of shoreline changes an indication of abrasion susceptibility. The results of such analysis can provide the basis for management and consideration in coastal area development. Therefore, this study identified and analyzed shoreline shifts and examined the effect of abrasion susceptibility on land cover changes in this coastal area using multitemporal Sentinel 2A imagery spanning from 2015 to 2020. The purpose of this research was to assess the effect of abrasion susceptibility in the coastal area of Bantul Regency with spatio-temporal approach to land cover and shoreline changes from 2015 to 2020. This research may be useful as a consideration to determine the development of coastal protection infrastructure, detailed coastal spatial planning, etc.

The systematic writing of this research is the first section discusses the background and research objectives. The second section discusses the study area and data specifications. The third section describes the research methodology, namely image pre-processing, spectral transformation: water index, digital shoreline analysis system (DSAS), land cover classification, and accuracy assessment of land cover classification. The fourth section discusses the main results of the research in the form of shoreline and land cover map from 2015 to 2020. The fifth section describes the shoreline and land cover dynamics, also the relationship between them, and the sixth section discusses the conclusions, limitations, and opportunities for further research.

2. Study Area and Data

2.1 Study Area

The study area is located between 110°12′ and 110°20′ E and between 7°59′ and 8°01′ S in the southern part of Bantul Regency, the southern coast of Special Region of Yogyakarta Regency, Indonesia (Figure 1). It is bordered by Kulonprogo Regency to the west, Gunungkidul to the east, and the Indian Ocean to the south. Bantul Regency has about 506.85 km^2 of land area with fertile lowland topography and less fertile hilly area covering more than half of it. The south coastal region has sandy natural conditions and some lagoons and stretches from Srandakan, Sanden, to Kretek District. The study area covers about 18.78 km^2, with elevations ranging from 0 to 10 m.a.s.l. or, in other words, falling into the category of the low-elevation coastal zone.

Mostly, the climate is wet tropical, with 25 days of rain in one month. In 2011, the highest rainfall was up to 44.5 mm/day. Other climatic parameters are as follows: the average wind speed ranges from 3 to 6 knots, the relative humidity varies from 30% to 97%, and the air temperature is in the range of 23°–34.77°C.

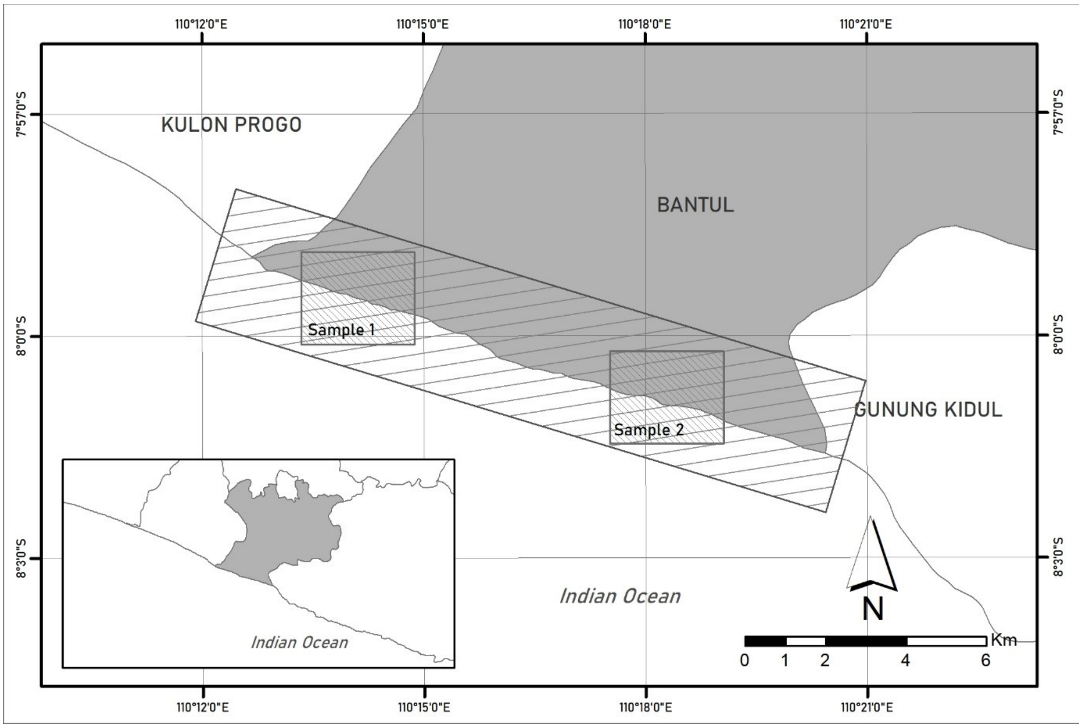

Figure 1: Study site in Bantul Regency, Indonesia

2.2 Analysis Procedure

In the previous study, there are several methods and techniques that can be used to extract shoreline from satellite imagery. Deepika et al., (2013) used GIS and statistical techniques to evaluate the shoreline change rate and cross-validation with root-mean-square error technique. Louati et al., (2014) and Haryani et al., (2019) used the band rationing that can be used to extract shoreline features from Landsat imageries. Bouchahma and Yan (2013) used cell-to-cell comparison of the binary image and measures changes based on Digital Shoreline Analysis System (DSAS) extension in ArcGIS. Biribo and Woodroffe (2013) measured historical shoreline changes by comparing shoreline positions over decades detected from aerial photograph or imagery, using tools such as Digital Shoreline Analysis System (DSAS) and software developed by United States Geological Survey (USGS). High Tide Line (HTL) (Mahapatra et al., 2014) has been interpreted from satellite data based on various geomorphological and land use/land cover features like land-ward berm/dune crest, sea-walls or embankment, permanent vegetation line, landward side of mangroves, beaches, salt pans, high-tidal mud flats and salt marshes. Seaward side of agricultural land etc. are also used.

Decision Tree is used because it is quite often utilized to classify land cover, land use, and other objects. Examples include land cover classification (Torma, 2013), land use and land cover classification (Kandrika and Roy, 2009), land cover classification in a heterogenous area (Verhulp and van Niekerk, 2017), wetland mapping (Berhane et al., 2018), and benthic habitat mapping of coral reef ecosystems (Wahidin et al., 2015). Otukei and Blaschke (2010) compared Decision Tree, Support Vector Machines, and Maximum Likelihood for Landsat 5 TM and Landsat 7 ETM+ to classify land cover in Kibale, Western Uganda. Decision Tree has higher overall accuracy than Support Vector Machine and Maximum Likelihood. For shoreline extraction, the water index transformation applied to Sentinel 2A imagery was converted using Otsu segmentation. Otsu can separate imagery into two classes with contrast differences. The boundary between dark and bright on imagery that has been transformed using water index can be identified as shoreline (Bangare et al., 2015). The land cover was classified using a Decision Tree with three hierarchical classifications based on three vegetation indexes (NDVI, EVI2, and GRVI). The Decision Tree used pixel values that represented every object in each vegetation index. Aerial photographs of several coasts were taken to determine the latest land cover and shoreline conditions.

2.3 Satellite Images

The spatial data used were satellite imagery and aerial photographs. Sentinel 2A images spanning from 2015 to 2020 were used to extract shoreline information and land cover change. They were recorded on December 26 (2015), April 24 (2016), May 19 (2017), May 14 (2018), May 29 (2019), and May 23 (2020). Despite the different recording times, they were taken in the same season, except for the 2015 image. This is because the Sentinel 2A image with the best condition (least cloud coverage) recorded in the same season in that year was not available for the study area.

3. Methodology

3.1 Image Pre-Processing

Sentinel-2A imagery (1C level) was pre-processed with atmospheric correction (2A level) using Sen2Cor on SNAP software. Then, cloud masking was applied to each downloaded image for every observation year using cloud data available in the directory (MSK_CLOUDS_B00.gml file).

3.2 Spectral transformation: Water Index

The modified normalized difference water index (MNDWI) (Xu, 2007) was used to distinguish water and non-water objects. The land and sea features on the Sentinel-2A images were separated by selecting a threshold based on the Otsu algorithm (Otsu, 1975) to create a distinct boundary between them. Wicaksono et al. (2019). McFeeters (1996), Ryu et al., (2002) and Pardo-Pascual et al., (2002) confirm that, for shoreline data extraction, water index transformation is easy to use and has a short processing time. The MNDWI transformation was computed using the formula below:

$$MNDWI = (B3 - B11) / (B3 + B11) \quad \text{Equation 1}$$

Where B3 = Green Band, B11 = SWIR1 Band of Sentinel-2A Imagery.

3.3 Digital Shoreline Analysis System (DSAS)

DSAS is a plugin on ArcMap used to calculate differences in shoreline positions (Himmelstoss et al., 2018). Shoreline data obtained from MNDWI transformation and Otsu threshold were refined using the Polynomial Approximation with Exponential Kernel (PAEK) with a tolerance of 100 m (Wicaksono et al., 2019). The DSAS transects were set at a length of 550 m and a distance of 50 m between transects; this setting was determined based on variations in shoreline shapes (Wicaksono and Winastuti, 2020). The End Point Rate (EPR) statistics on DSAS was used to calculate the change rate of the shoreline transformed (y-axis, MNDWI) from 2015 to 2020 (in meters). Afterward, the EPR was classified according to the abrasion damage level characterized by the Center for Water Research and Development (Puslitbang Pengairan) (Table 1). The damage level is termed as abrasion susceptibility (Center for Water Research and Development, 1992, PSBA, 2017 and Wicaksono et al., 2019).

Table 1: Damage level classifications based on shoreline change rates

Damage levels	Shoreline Change Rates (in meter)
Low	< 0.5 m/year
Moderate	0.5 – 2.0 m/year
High	2.0 – 5.0 m/year
Very High	5.0 – 10.0 m/year
Extremely High	> 10.0 m/year

Source: Center for Water Research and Development (Center for Water Research and Development, 1992)

3.4 Land Cover Classification

The vegetation index was developed to characterize vegetation and non-vegetation land covers using a combination of two or more spectral channels associated with photosynthesis (Huete et al., 1999). A high vegetation index value indicates a level of greenness that reflects plants with high activities and low stress levels, and vice versa (Rocha and Shaver, 2009). Therefore, this index is widely applied to analyses related to changes in land cover and vegetation. In this research, the Normalized Difference Vegetation Index (NDVI), Two-band Enhanced Vegetation Index (EVI2), and Green-Red Vegetation Index (GRVI) were used to classify land cover objects.

NDVI is relatively more sensitive to the presence of chlorophyll pigments, while EVI2 is more related to changes in canopy structure, such as the Leaf Area Index (LAI), vegetation type, and vegetation physiognomy. Both complement each other in global vegetation studies and enhance vegetation change detection and extraction of biophysical canopy parameters (Huete et al., 2002). GRVI is used more often to evaluate forest degradation and tree canopy phenology because its green channel is particularly sensitive to leaf color change on the canopy surface (Motohka et al., 2010). Below are the formulas used to classify the land cover.

$$NDVI = (B8A – B4) / (B8A + B4) \quad \text{Equation 2}$$

$$EVI2 = 2.5 * (B8A – B4) / (B8A + 2.4 * B4 + 1) \quad \text{Equation 3}$$

$$GRVI = (B3 – B4) / (B3 + B4) \quad \text{Equation 4}$$

Where B3 = Green Band, B4 = Red Band, B8A = NIR Band of Sentinel-2A Imagery.

The Decision Tree used for land cover classification in this study was already available in ENVI software. It is a category of machine learning applicable to classifying large amounts of data (Hastie et al., 2009) because of its computational simplicity, which is useful for satellite imagery analysis performed on thousands or millions of pixels (Holloway et al., 2019). The Decision Tree uses "if, then" algorithm, meaning that if an object matches the given argument, then it belongs to that predetermined class. In this research, the argument was built on the pixel value of each land cover for every vegetation index transformation performed. The Decision Tree that used can be seen in Figure 2. The pixel values used in the Decision Tree were determined by first selecting training area polygons for every land cover type resulting from each vegetation index transformation. The pixel value was the average of total pixel values included in the training area of each land cover. The training polygons had a total area of 0.083 to 0.570 km^2, of which the smallest was built-up land, whereas the largest was water body. The built-up land was given more training polygons to compensate for the smallest area.

3.5 Accuracy Assessment of Land Cover Classification

The land cover classification obtained from the 2020 image was assessed for accuracy because the process involved observing the actual land cover on-site, which was only possible during the research time, 2020. During this on-site validation, land cover data were collected at the coordinates of the predetermined samples.

4. Results

Figure 3 and 4 show shoreline changes, including both accretion and abrasion, in the study area. The widest accretion occurred from 2016 to 2017, creating an additional area of 22.32 ha, whereas the least significant accretion was from 2019 to 2020, adding 0.28 ha of land to the coastal region. Meanwhile, the most severe abrasion was detected from 2019 to 2020, leading to an area loss of 34.89 ha, whereas the least severe one was from 2016 to 2017, reducing the coastal area by 2.41 ha.

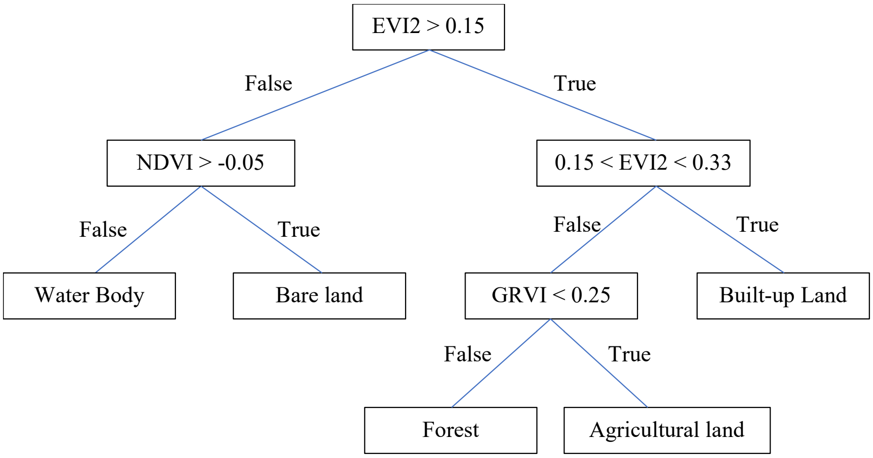

Figure 2: Decision tree used to classify land cover from Sentinel 2A imagery

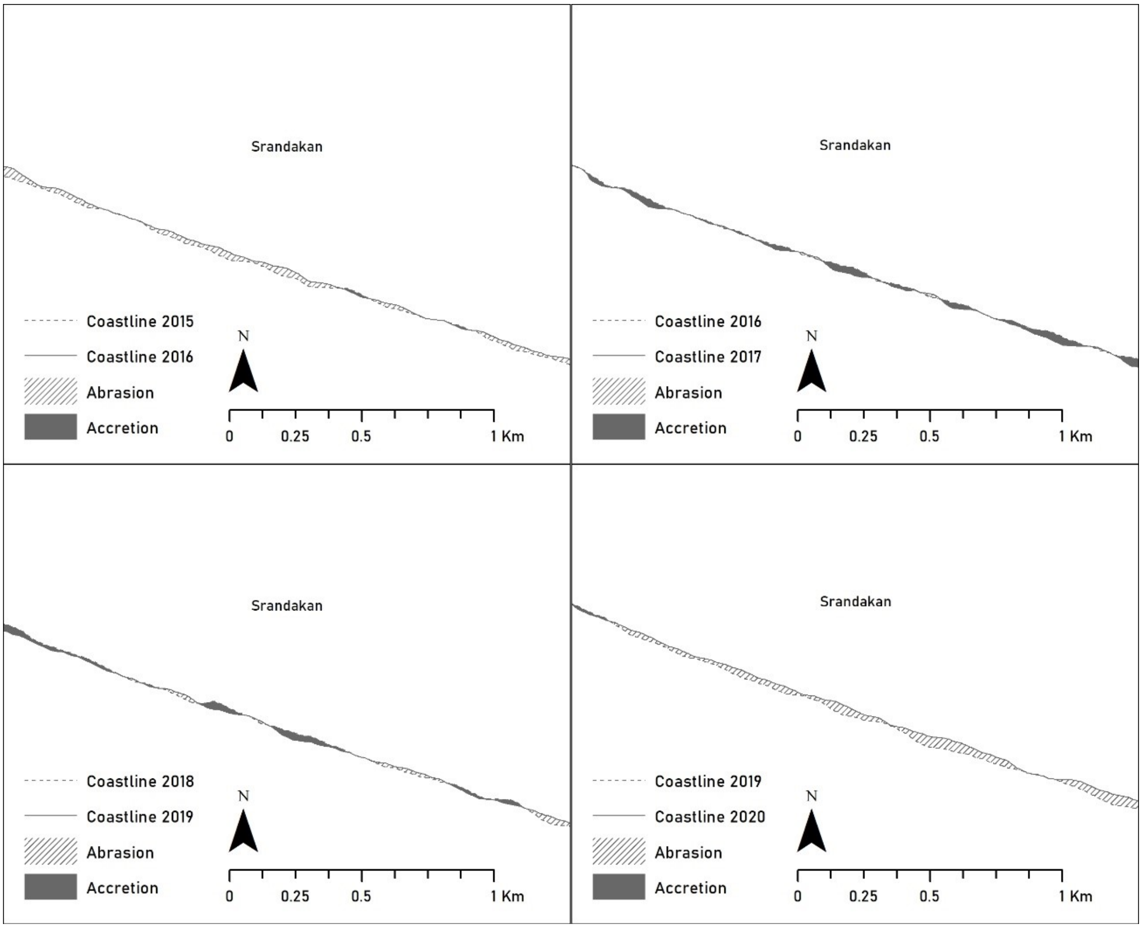

Figure 3: The result of shoreline extraction indicating accretion and abrasion (Sample 1)

From 2015 until 2020, the total areas subjected to accretion and abrasion were 1.13 ha and 33.29 ha, respectively. According to the transect data, the shoreline abrasion rate was in the range of 0.21–41.58 m/year, with an average of -6.20 m/year. Figure 5-10 show the distribution of land cover classification, as interpreted from Sentinel 2A imagery, and Table 2 presents the matrix of land cover classification accuracy in 2020. From the classification results, the area values for water body, forest, agriculture, built-up land, and bareland in 2015 are 42.94 ha, 0.49 ha, 20.41 ha, 72.26 ha, and 13.58 ha consecutively. For 2016 the areas are 31.80, 0.32 ha, 39.09 ha, 93.56 ha, and 115.77 ha.

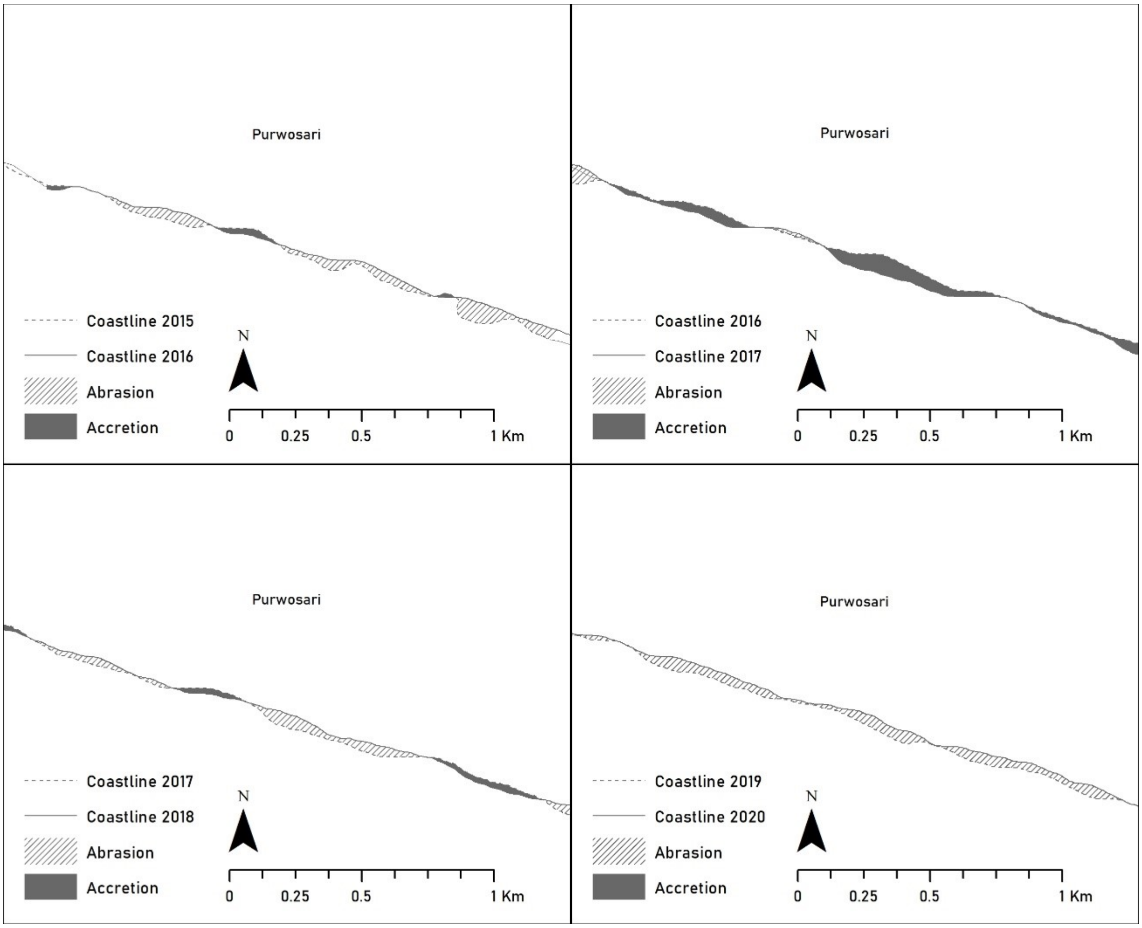

Figure 4: The result of shoreline extraction indicating accretion and abrasion (Sample 2)

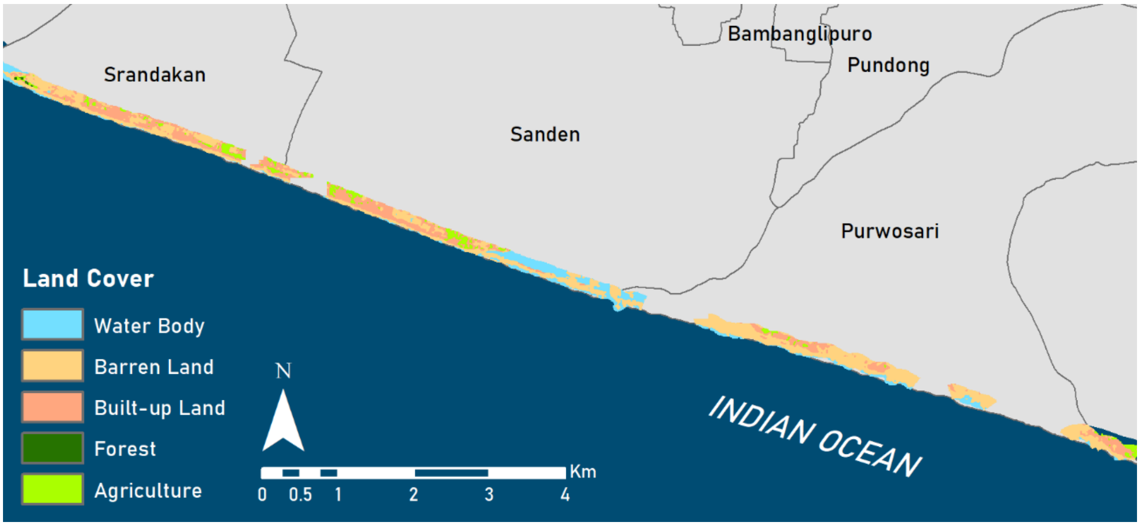

Figure 5: Land cover of the study area in 2015, as identified using decision tree classification

For 2017 the areas are 31.09 ha, 8 ha, 50.31 ha, 81.09 ha, and 159 ha. For 2018 the areas are 35.83 ha, 0.16 ha, 19.86 ha, 98.89 ha, and 176.42 ha. For 2019 the areas are 30.65 ha, 0.02 ha, 21.97 ha, 93.6 ha, and 181.95 ha. For 2020 the areas are 35 ha, 4.14 ha, 34.1 ha, 116.62 ha, 136.73 ha.

Figure 12–19 show beach cross-profile with a length of 100 meter from the shoreline with land covers on that beach. More detailed information regarding the characteristics of every beach in this study can be seen on Table 10-17.

Table 2: Accuracy of the land cover classification in 2020

		Classification Results					
		Water Body	Forest	Agricultural Land	Built-Up Land	Bare Land	Producer Accuracy (%)
Check	Water Body	31	1	0	1	2	88.57
	Forest	0	29	0	0	0	100.00
	Agricultural Land	0	9	23	0	3	65.71
	Built-Up Land	1	0	3	29	2	82.86
	Bare Land	0	4	1	3	27	77.14
	User Accuracy (%)	96.87	67.44	85.18	87.88	79.41	82.25

Table 3: Matrix of land cover change from 2015 to 2016 (in meter^2)

		2016				
		Water Body	Forest	Agricultural Land	Built-Up Land	Bare Land
2015	Water Body	181,000	0	200	8,800	76,600
	Forest	0	400	4,100	200	200
	Agricultural Land	200	100	106,500	58,000	6,400
	Built-Up Land	1,800	2,500	134,700	465,700	77,300
	Bare Land	83,200	0	47,400	225,300	718,100

Table 4: Matrix of land cover change from 2016 to 2017 (in meter^2)

		2017				
		Water Body	Forest	Agricultural Land	Built-Up Land	Bare Land
2016	Water Body	129,600	0	0	1,900	154,300
	Forest	0	2,300	0	500	0
	Agricultural Land	0	50,000	222,800	61,600	14,500
	Built-Up Land	2,600	3,000	188,900	515,600	128,000
	Bare Land	56,800	100	4,900	127,800	898,700

Table 5: Matrix of land cover change from 2017 to 2018 (in meter^2)

		2018				
		Water Body	Forest	Agricultural Land	Built-Up Land	Bare Land
2017	Water Body	141,700	0	0	100	87,700
	Forest	100	900	57,600	19,100	800
	Agricultural Land	200	0	111,500	372,800	9,800
	Built-Up Land	1,000	0	6,300	499,200	276,400
	Bare Land	151,200	0	1,800	27,700	1,252,600

Table 6: Matrix of land cover change from 2018 to 2019 (in meter^2)

		2019				
		Water Body	Forest	Agricultural Land	Built-Up Land	Bare Land
2018	Water Body	196,200	0	0	900	119,700
	Forest	0	0	500	0	0
	Agricultural Land	0	200	13,900	29,600	2,800
	Built-Up Land	0	0	75,600	732,300	83,600
	Bare Land	50,100	0	1,800	162,000	1,439,700

Table 7: Matrix of land cover change from 2019 to 2020 (in meter^2)

		2020				
		Water Body	Forest	Agricultural Land	Built-Up Land	Bare Land
2019	Water Body	184,300	0	200	1,900	45,300
	Forest	0	0	200	0	0
	Agricultural Land	4,300	19,000	137,100	54,500	3,600
	Built-Up Land	12,200	3,100	126,000	737,200	56,700
	Bare Land	100,800	600	5,100	224,500	1,170,800

Table 8: RMSE and uncertainty of Sentinel-2A shorelines

Date (mm/dd/yyyy)	Horizontal RMSE (m)	Uncertainty (in meter)			Total Uncertainty
		Geometric Accuracy RMSE	Pixel Size	Horizontal Offset of Tides	
12/26/201	64.96	6.64	20	1.37	28.01
05/19/2017	39.3	8.20	20	13.84	42.04
05/29/2019	32.84	6.69	20	2.52	29.21
05/23/2020	40.19	5.76	20	19.61	45.37

* In 2016 and 2018 there is no validation because of lack of aerial photograph

Table 9: Various vegetation species in Bantul coastal area

No.	Name	Latin Name
1.	Hibiscus / sea hibiscus / coral tree	*Hibiscus tiliaceus*
2.	Crown flower	*Calotropis gigantea*
3.	Palmyra palm	*Borrasus flabellifer*
4.	Bayhops / beach morning glory / goat's foot	*Ipomoea pes-caprae*
5.	Shaggy buttonweed	*Spermacoce hispida*
6.	Shrubby false buttonweed (herbs)	*Spermacoce verticillata*
7.	Ravan's Moustache	*Spinifex littoreus*
8.	Bay bean	*Canavalia rosea*
9.	Grasses	*Cyperus spp. Fimbrystilis dichotoma*
10.	Screwpine	*Pandanus tectorius*
11.	Crabgrass	*Digitaria sp.*

Source: Environment and Forestry Service (DLHK) of the Special Region of Yogyakarta

Table 10: Cross-profile descriptions of Pandansimo Beach

Pandansimo Beach	
Position	X: 413888.893, Y: 9116959.231
Shoreline change rate	+5.03 m/year
Ridge slope	6°
Landform	Beach ridge
Genesis	Marine
Flora	*Casuarina equisetifolia*
Cultural Landscape	Wild fisheries
Settlement Pattern	Linear to the beach
Economy	Capture fishery
Socio-culture	Group of fishers
Land cover	Settlements, Shrubs
Land planning	Coastal Setback, Tourism, Agricultural land, Power Plant, Trade and Services

Table 11: Cross-profile descriptions of Baru beach

Baru Beach	
Position	X: 414447.165, Y: 9116758.147
Shoreline change rate	+1.43 m/year
Ridge slope	1°
Landform	Beach ridge
Genesis	Marine
Flora	*Casuarina equisetifolia*
Cultural Landscape	Tourism
Settlement Pattern	Linear to the street
Economy	Trades
Socio-culture	Group of merchants
Land cover	Trading
Land planning	Coastal Setback, Tourism, Trade and Services

Table 12: Cross-Profile Descriptions of Kuwaru Beach

Kuwaru Beach	
Position	X: 415164.188, Y: 9116562.355
Shoreline change rate	+4.9 m/year
Ridge slope	11°
Landform	Beach, Beach Ridge
Genesis	Marine
Flora	*Casuarina equisetifolia*
Cultural Landscape	Aquaculture
Settlement Pattern	none
Economy	Fish farming
Socio-culture	Aquaculture company
Land cover	Pond, Unused Land
Land planning	Coastal Setback, Tourism, Agricultural land, Power Plant, Trade and Services

Table 13: Cross-Profile Descriptions of Pandansari Beach

Kuwaru Beach	
Position	X: 415164.188, Y: 9116562.355
Shoreline change rate	+4.9 m/year
Ridge slope	11°
Landform	Beach, Beach Ridge
Genesis	Marine
Flora	*Casuarina equisetifolia*
Cultural Landscape	Aquaculture
Settlement Pattern	none
Economy	Fish farming
Socio-culture	Aquaculture company
Land cover	Pond, Unused Land
Land planning	Coastal Setback, Tourism, Agricultural land, Power Plant, Trade and Services

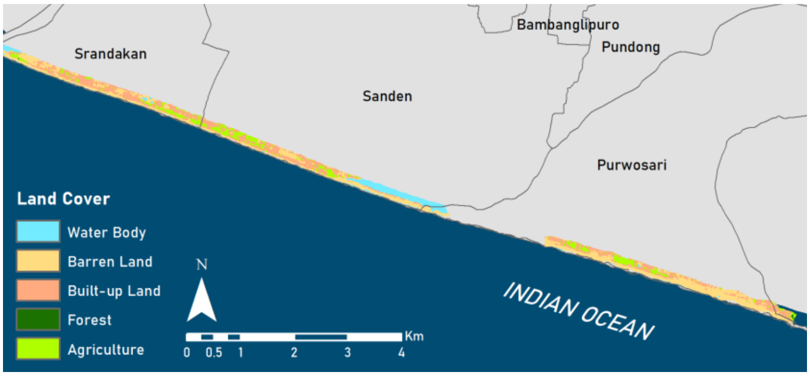

Figure 6: Land cover of the study area in 2016, as identified using decision tree classification

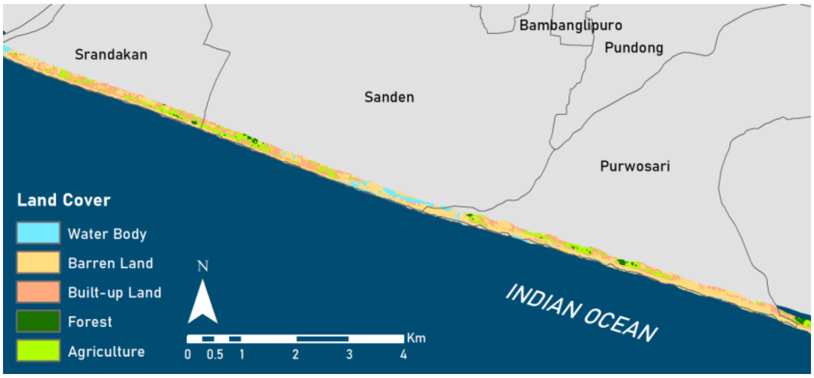

Figure 7: Land cover of the study area in 2017, as identified using decision tree classification

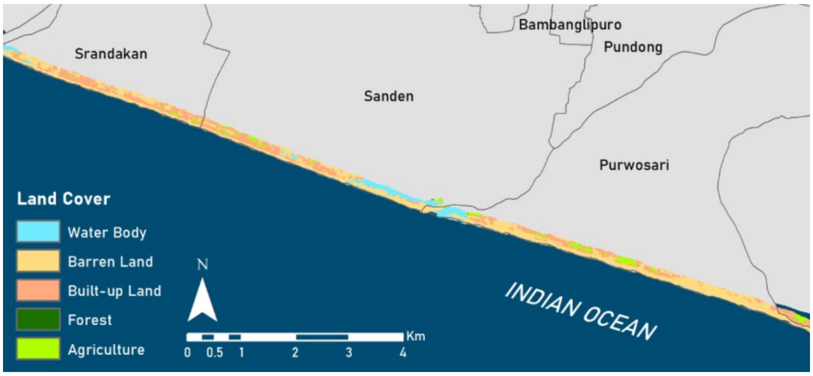

Figure 8: Land Cover of the Study Area in 2018, as Identified using Decision Tree Classification

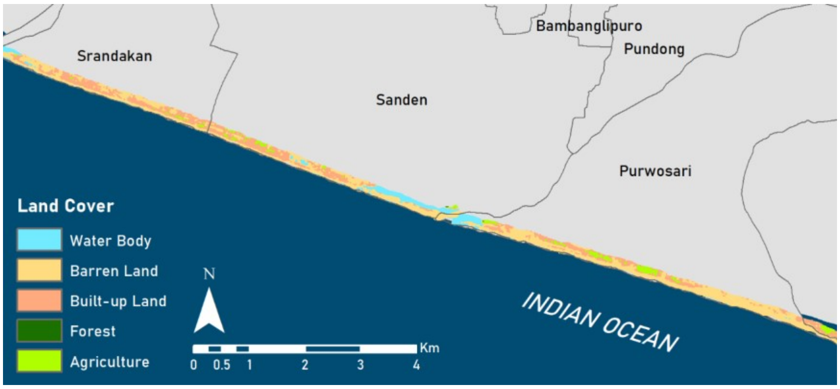

Figure 9: Land Cover of the Study Area in 2019, as Identified using Decision Tree Classification

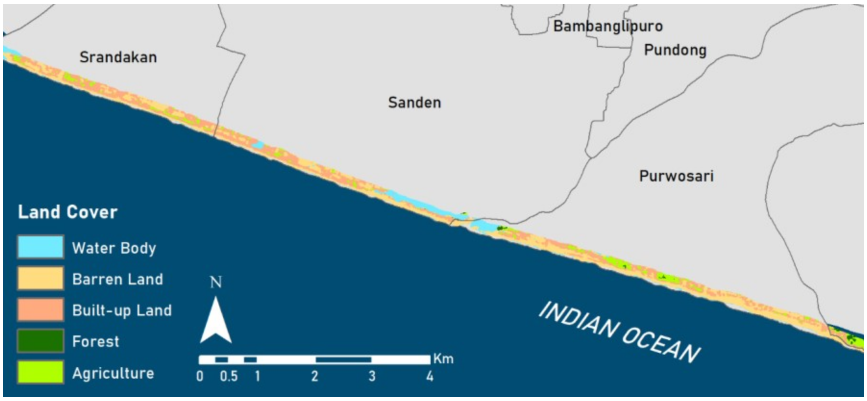

Figure 10: Land cover of the study area in 2020, as identified using decision tree classification

Figure 11: Aerial image acquisition and cross-profile locations

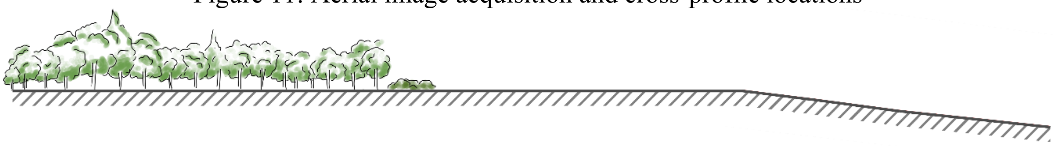

Figure 12: Cross-profile of Pandansimo Beach

Figure 13: Cross-profile of Baru Beach

Figure 14: Cross-profile of Kuwaru Beach

Figure 15: Cross-profile of Pandansari Beach

Pandansimo Beach has shoreline change rate about +5.03 m/year with 6° ridge slope. Most of land cover in Pandansimo Beach is settlements and shrubs, the settlements position is linear to the beach and most activities in this beach is capture fisheries. Baru Beach has shoreline change rate about +1.43 m/year with 1° ridge slope. This beach mostly utilized as a tourism with many merchants, found little to no settlements in this beach. Kuwaru Beach has shorline change rate about +4.9 m/year with 11° ridge slope. There is no settlement in this beach because mostly utilized as a fish farming place with ponds scattered around the area. Pandansari Beach characteristics more or less is just the same as Kuwaru Beach. Most of its land covers are ponds that is used as fish farming. There is no settlement in this beach because tourism become the main activity of this beach. Samas Beach has shoreline change rate about +1.59 m/year with 4° ridge slope. There are grouped settlements in this beach with merchants and fishers as the inhabitants main activities. The east side of Samas Beach is Opak River estuary which also adjacent to Depok Beach. Depok Beach has shoreline change rate -30.36 m/year with 11.5° ridge slope. The inhabitants of this beach mostly borks as capture fishing fishers and merchants because this beach is utilized as tourism too. Pelangi Beach has shoreline change rate -7.73 m/year with 14.5° ridge slope. This beach has no settlement or any other land cover except unused lands and shrubs. Tourism is the main activity in Pelangi Beach. Parangkusumo Beach has shoreline change rate -7.57 m/year with 5° ridge slope. This beach is one of the main tourism attraction in Bantul Regency. Most activities in Parangkusumo Beach is tourism with settlements and merchants scattered across the beach. Most of flora found on beaches in this study is *Casuarina equisetifolia*, but there are another flora on some beaches, like *Ipomoea pes-caprae* on Samas Beach, *Spinifex littoreus* on Pelangi Beach and Parangkusumo Beach, and *Borrasus flabellifer* on Parangkusumo Beach.

5. Validation of Results

MNDWI shoreline in this study is the result of research by Wicaksono et al., (2021) with RMSE and uncertainty values shown in Table 8. which gives better results than the AWEInsh, AWEIsh, B11, B3/B11 Ratio, and NDWI methods. Shoreline validation is done by calculating the accuracy of horizontal geometry (distance difference in meter between shoreline extraction from satellite and aerial photograph validation), which has already considered the tidal correction. Further detail related to the method of geometric accuracy assessment of shoreline extracted from imagery can be seen in the study of Wicaksono and Wicaksono (2019), and Wicaksono et al., (2021). Unavailable field data as comparison creates an obstacle for this study so that the shoreline data is validated through visual interpretation of aerial photograph with spatial resolution of 0.3 meter.

6. Discussion

Table 3-7 show land cover changes in the coastal area of Bantul Regency for at least the last six years (2015 – 2020). There are five land cover types: bare land, built-up land, agricultural land, forest, and water body. Here, land cover changes are presented using cross-tabulation to see the trend of change annually. The most significant change within the course of six years was the conversion of bare land to built-up land, affecting an area of 271,700 m^2. Bare land is any empty land with no coverage nor socioeconomic activities in place. In coastal areas, it is always affected by tides and may differ based on its proximity to the sea, but behind the coast, it is composed of sand with some vegetation cover like herbs and shrubs.

Apart from bare land, agricultural land was also largely converted to non-agricultural uses within six years. Agricultural land is any land utilized for, in this case, farming and producing two commodities developed in this area: chilies and shallots. Cultivation practices are mostly carried out in coastal areas not used for tourism activities, especially in parts that are not too close to the coast to avoid high tides. This agricultural land is also usually adjacent to the forest, which is dominated by woody plants with medium to high density. Table 9 lists vegetation species growing in the coastal area of Bantul Regency.

Beach tourism has long been a leading regional sector that brings in a high number of tourists (Tourism Services of Bantul Regency, 2019). This sector management often creates new tourism objects in several spots that have not been previously managed, but their emergence is also followed by failure to preserve existing beaches. Losing in a competitive term is the main reason some beaches are no longer cared for tourism purposes and abandoned. These dynamics create a major influence on land-use change, especially the conversion of different land-use types into built-up land, e.g., restaurants and various tourism amenities such as toilets, information centers, and souvenir centers. In the study area, water bodies include lagoons, a pool of waters bordered by beach ridge and scattered in several beaches—providing features or characteristics for identification. Lagoons create a swimming area for visiting tourists of varying age ranges because there are swimming restrictions in the sea for every beach in the Special Region of Yogyakarta. The underlying reason is that the coastal areas in this region border the Indian Ocean and are, therefore, faced with high and destructive waves. For this reason, beach managers or investors utilize lagoons or provide pools for tourists, especially children.

Coastal dynamics are influenced by natural processes and accelerated by human activities (Sunarto, 2004). Natural/hydrodynamic processes involved are waves, winds, and currents. Human activities in coastal areas can affect natural processes. Shoreline changes depend on the equilibrium between nearshore sediment motion by waves and currents (Triatmodjo, 2008), topography (Sinaga and Susiati, 2007), coastal material, tides, and wind (Dulbahri, 1983). Coastal morphodynamics is part of a coastal geomorphological study covering shoreline shifts in a period of time and their causes, coastal processes and their impact on the coast itself, and sources and patterns of coastal sediment movement (Bird, 2008). Coastal geomorphology is also closely related to beach or coastal typology.

Various studies have been conducted at different scales, but mostly local; hence, improved management at the regional level is necessary. Alves et al., (2020) state that only regional solutions and adaptive approaches at multiple scales are appropriate and effective for coastal management. For this reason, after reviewing regional coastal dynamics, more detailed observations were made in several places that experienced significant shoreline changes through aerial photography and cross-sectional profiles on several beaches: Pandansimo, Baru, Kuwaru, Patihan, Samas, Depok, Pelangi, and Parangkusumo Beach (Figure 11). The cross-profile method, as proposed by Marfai (2011), consists of cross-sections of land cover along with the description of their respective geo-ecological factors: land cover, landforms, and disasters and their ecological and environmental impacts, with a transect length of about 5 km.

Coastal disaster risk is associated with the danger of floods, high winds and waves, coastal erosion, storms, and human development along the coast (Thior et al., 2019). Hydrodynamic factors like wind, waves, and currents are natural forces that easily remove and carry unconsolidated materials (i.e., sand), causing changes in shoreline position through erosion, transportation, and sedimentation. The likelihood of a disaster occurrence will vary from one place to another depending on geomorphological variables, weather conditions, topography-bathymetry, and land cover/use arrangement so that disaster mitigation measures will also differ spatially. Therefore, the physical, social, economic, and spatial conditions that can affect abrasion and act as elements exposed to this process are described in each cross-section. Characterizing waves at Kuwaru Beach during eastern monsoon, Mutaqin et al., (2014) found that almost all waves are constructive with typical larger swash than the back swash, long wavelength, and low wave height and frequency. They mostly occur in dry season and are responsible for adding sediments to build up the coast. Malawani et al., (2019) examined the coastal response to tidal waves induced by cyclones in the Special Region of Yogyakarta and found that they were influenced by coastal typology and the width and slope of the ridge. The existence of lagoons can inhibit the arrival of tidal waves and capture the backflow. Eroding waves can happen sporadically and form small bays that create a center of rip currents, such as those on Depok Beach (Freksi and Srijono, 2013). Beach with flat slopes and narrow ridges are prone to tidal waves. Saputro et al., (2017) investigated the relationship between coastal typology and shoreline changes in Bantul Regency and revealed three reasons behind shoreline shifts: sandy beaches, facing directly to the ocean, and availability of material supply from the upstream. The coastal typology in Bantul Regency consists of sandy beaches, rocky beaches, and beaches of mixed sand and mud.

Pandansimo, Baru, and Kuwaru Beach are adjacent to each other and have similar physical conditions but different social and economic characteristics. Pandansimo has fishing settlements, Baru is a place of services and trades that support beach tourism, and Kuwaru is utilized as industrial ponds managed by several companies. Based on the analysis result of remote sensing imagery in six years (2015–2020), the shoreline changes on the three beaches show a trend of accretion. However, there is some evidence showing signs of abrasion in the field, as indicated by the ridge slope and abandoned buildings. Mutaqin (2017) states that from 1995 to 2015, the shoreline at Kuwaru experienced a landward retreat of more than 50 m. In addition to massive abrasion that has damaged human settlements around the coast of Samas Beach, there is also a trend of accretion caused by sand blocking the estuary of Opak River and, thus, forming lagoons that prevent river water from flowing into the sea (Choirunnisa and Giyarsih, 2018). Figure 23 shows human settlements on Samas Beach threatened by extreme waves and overflows from the estuary.

Table 14: Cross-profile descriptions of Samas Beach

Samas Beach	
Position	X: 419057.539, Y: 9115089.285
Shoreline change rate	+1.59 m/year
Ridge slope	4°
Landform	Beach, Barrier Beach
Genesis	Fluvio-Marine
Flora	*Casuarina equisetifolia, Ipomoea pes-caprae*
Cultural Landscape	Settlements, Tourism, Wild Fisheries
Settlement Pattern	Grouped
Economy	Trades, Capture fishery
Socio-culture	Group of fishers
Land cover	Settlements, Trading, Unused Land
Land planning	**Coastal Setback, River Setback, Agricultural land, Low-Density Housing**

Table 15: Cross-profile descriptions of Depok Beach

Depok Beach	
Position	X: 423345.782, Y: 9113755.782
Shoreline change rate	-30.36 m/year
Ridge slope	11.5°
Landform	Beach
Genesis	Fluvio-Marine
Flora	*Casuarina equisetifolia*
Cultural Landscape	Settlements, Tourism, Wild Fisheries
Settlement Pattern	Linear to the Beach
Economy	Trades, Capture fishery
Socio-culture	Group of Fishers
Land cover	Trading, Settlements
Land planning	Coastal Setback, Natural Reserve, Low-Density Housing, Transportation

Table 16: Cross-profile descriptions of Pelangi Beach

Pelangi Beach	
Position	X: 421741.742, Y: 9114205.575
Shoreline change rate	-7.73 m/year
Ridge slope	14.5°
Landform	Beach, Beach Ridge
Genesis	Marine, Aeolian
Flora	*Casuarina equisetifolia, Spinifex littoreus*
Cultural Landscape	Tourism
Settlement Pattern	None
Economy	None
Socio-culture	-
Land cover	Unused Land, Shrubs
Land planning	Coastal Setback, Natural Reserve

Table 17: Cross-Profile Descriptions of Parangkusumo Beach

Parangkusumo Beach	
Position	X: 425535.214, Y: 9113127.395
Shoreline change rate	-7.57 m/year
Ridge slope	5°
Landform	Beach, Sand Dunes
Genesis	Marine, Aeolian
Flora	*Casuarina equisetifolia, Spinifex littoreus, Borrasus flabellifer, Spinifex littoreus*
Cultural Landscape	Settlements, Tourism
Settlement Pattern	Grouped
Economy	Trades
Socio-culture	Group of Merchants
Land cover	Trading, Settlements
Land planning	Coastal Setback, Natural Reserve, Tourism

Abrasion tends to occur at varying degrees in Pandansari, Depok, Pelangi, and Parangkusumo Beach. Generally, beaches subjected to abrasion have a slightly steep ridge slope (>8.1°) and, based on field observation, collapsed vegetation and damaged buildings—which are believed to have been caused by extreme waves. Depok requires more attention because it experiences the most severe abrasion compared to other beaches, particularly because it is a tourist attraction known for its culinary and fish auction market. Likewise, Parangkusumo is a tourist attraction famous for its natural and historical beauty. Figure 12-19 show the cross-profile of beaches with some of the land cover. The description of each cross-profile is shown by Table 10-17. The 2020 aerial photography provides existing land cover types and their distance to the shoreline.

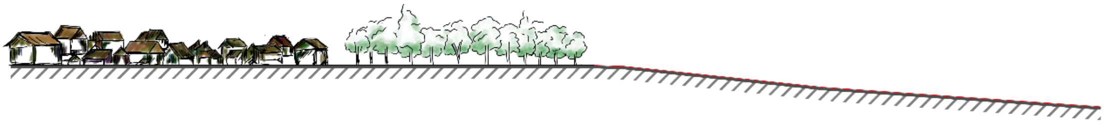

Figure 16: Cross-profile of Samas Beach

Figure 17: Cross-profile of Depok Beach

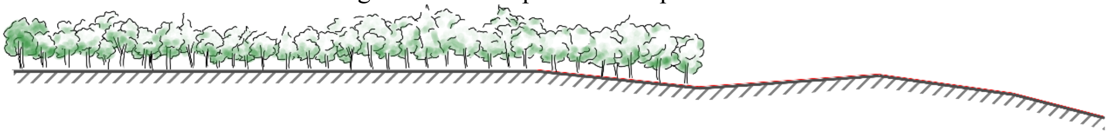

Figure 18: Cross-profile of Pelangi Beach

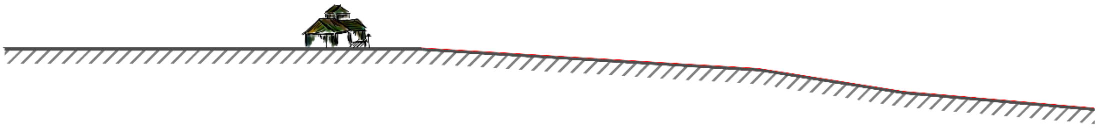

Figure 19: Cross-profile of Parangkusumo Beach

Figure 20 shows the condition of Pandansimo Beach and its surroundings, can be seen that the settlements are in relatively close distance to the shoreline: about 27 m and adjacent to the ponds. Figure 21, presenting the condition of Baru Beach and its surroundings, shows an almost similar condition with Pandansimo Beach, the settlement/trade buildings are in relatively close distance to the shoreline: about 20 m and adjacent to the ponds. Meanwhile, Figure 22 shows illegal beach sand mining at the estuary of Opak River. Figure 24-26 show the condition of Depok and Cemara Sewu Beach and its surroundings, including tourist sites that are close to the shoreline, cypresses and sandbanks as natural barriers, and ponds around the sandbanks that have turned green.

Based on the results, there is no causal relationship between abrasion and coastal land cover. What affects the abrasion is sand mining practices in river estuaries and upstream that decrease sand supply to the beach and result in a new balance. However, it is essential to study changes in shoreline and land cover because their impact can only be managed by observing and monitoring the condition of existing land cover as an exposed element. Van Westen et al. (2006) explain that at-risk elements are all objects, people, animals, and activities or processes, including buildings, public facilities, populations, economic activities, and the environment, affected by a disaster in a place, either directly or indirectly.

The research output offers a basis for increasing anthropogenic interventions and actions on climate change by local policy stakeholders in this shared ecosystem. Various mitigation options for coastal abrasion are, for example, hard engineering solutions (breakwaters, groins, seawalls, jetties, revetments, dikes, storm surge barriers, and closure dams) and soft engineering solutions (beach nourishment, natural area (dune and mangrove) restoration, fluvial sediment management, land claim, ecosystem-based management, cliff stabilization) (Giardino et al., 2018).

However, hard engineering solutions usually alter the natural environment of the coast, resulting in negative impacts. With current and future environmental conditions to consider, a more adaptive, sustainable, multi-functional, and economically viable coastal protection strategy is thereby needed to help overcome current and predicted coastal erosion problems. Approaches based on natural ecosystems, such as wetlands, reef structures, seagrass beds, and sand dune vegetation, offer optimal natural alternatives to tackle coastal erosion. Coastal ecosystems can self-repair and restore and provide significant advantages for hard engineering approaches to deal with coastal erosion (Gracia et al., 2018). Ecosystem-based coastal erosion management can provide a better, more cost-effective, sustainable, and environmentally based alternative to conventional management techniques.

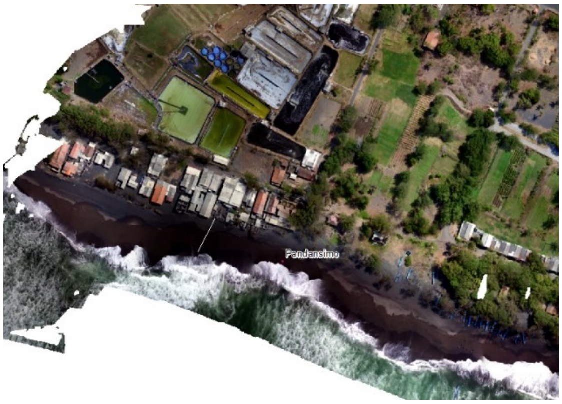

Figure 20: Settlements located close to the shoreline (only about 27 m apart) and adjacent to ponds in Pandansimo Beach.

Figure 21:Fairly Close distance between the trade area and the shoreline (Only about 21 m) in Baru Beach

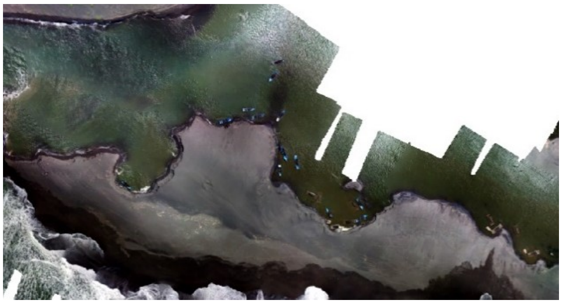

Figure 22: Beach sand mining activity (materials transported using boats) in the estuary of Opak River

Figure 23: Settlements that are located rather far from the shoreline (about 90 m apart) but near the lagoon of Samas Beach

Figure 24: The trade area and fish auction market that are located about 65 m from Depok Beach

Figure 25: Ponds that are Located among Sand Dunes at Depok Beach

Figure 26: Sand dunes and Casuarina equisetifolias scattered throughout the Cemara Sewu Beach

These advantages include, among others, nature conservation, recreational space provision, carbon storage, water quality enhancement, and fishery production. However, the developments of an ecosystem and its ability depend on the coast's characteristics, hydrodynamics, structure, habitat, and the destructive level of coastal erosion.

7. Conclusions

There is no causal relationship between coastal abrasion in Bantul Regency and land cover changes. Nevertheless, the land cover changed in the course of six years (2015–2020), with bare land being the most largely converted to built-up land (27.17 ha), indicating increasing anthropological activities from year to year. Sand mining in the estuary and upstream is among the human activities that influence abrasion in the coastal areas observed. The correlation between shoreline and land cover change needs to be further studied because, to manage shoreline shifts and their impact, the responsible parties should understand the existing land cover condition because it is an object exposed to shoreline dynamics. Long-term mitigation strategies against climate change-induced disasters need to be implemented immediately to maintain the physical condition and land cover in the coastal regions to enhance their resilience.

Acknowledgements

This research was funded by Gadjah Mada University Final Project Recognition scheme in the 2020. The authors would like to thank to Fajrun Wahidil Muharram, S.Si. and Yuniarsita Setyo Wulandari, S.Si. as employees at Parangtritis Geomaritime Science Park who helps to provide aerial photography of Parangtritis Village, Bantul Regency. Thank you also to Yanuar Sulistyaningrum, S.Pd., M.Sc. who has assisted in research administration.

References

Alves, B., Angnuureng, D. B., Morand, P. and Almar, R., 2020, A Review on Coastal Erosion and Flooding Risks and Best Management Practices in West Africa: What has been done and should be done. *Journal of Coastal Conservation*, Vol. 24(38), 1-22.

Bangare, S. L., Dubal, A., Bangare P, S., and Patil, S. T., 2015, Reviewing Otsu's Method for Image Thresholding. *International Journal of Applied Engineering Research*, Vol. 10(9), 21777 - 21783

Berhane, T, M., Lane, C. R., Qiusheng, W., Autrey, Oleg, B. C., Anenkhonov, A. and Chepinoga, V. V., 2018, Decision-Tree, Rule-Based, and Random Forest CLassification of High-Resolution Multispectral Imagery for Wetland Mapping and Inventory. *Remote Sensing*, Vol. 10(4).

Bird, E. C. F., 2008, *Coastal Geomorphology: An Introduction*, 2nd Edition, (London: Wiley).

Biribo, N. and Woodroffe, C. D., 2013, Historical Area and Shoreline Change of Reef Islands around Tarawa Atoll, Kiribati. *Sustainability Science,* Vol. 8(3), 345–362.

Bouchahma, M. and Yan, W., 2013, Monitoring Shoreline change on Djerba Island Using GIS and Multi-Temporal Satellite Data. *Arabian Journal of Geosciences,* Vol. 7(9), 3705–3713.

Center for Water Research and Development, 1992, *Beach and Estuary Damages in Indonesia [Kerusakan Pantai dan Muara di Indonesia]*. (Bandung: CWRD).

CERC, 1984, *Shore Protection Manual Volume I*, 4th, (Washington: U.S. Army Coastal Engineering Research Center).

Choirunnisa, A. K. and Giyarsih, S. R., 2018, The Socioeconomic Vulnerability of Coastal Communities to Abrasion in Samas, Bantul Regency, Indonesia. *Quaestiones Geographicae*, Vol. 37 (3): 115-126.

Deepika, B., Avinash, K. and Jayappa, K. S., 2013, Shoreline Change Rate Estimation and its Forecast: Remote Sensing, Geographical Information System and Statistics-Based Approach. *International Journal of Environmental Science and Technology*, Vol. 11(2), 395–416.

Dulbahri, 1983, *Application of 1:250,000 Landsat images for Shoreline Change Studies in Central and Eastern Java Island [Aplikasi Citra Landsat skala 1:250.000 untuk Studi Perubahan Garis Pantai di Daerah Jawa Tengah dan Jawa Timur],* (Yogyakarta: Faculty of Geography, Universitas Gadjah Mada).

Freski, Y. R. and Srijono, 2013, Coastal Abrasion Mechanism in Depok Beach, Bantul, the Special Region Yogyakarta [Mekanisme Abrasi Pesisir di Kawasan Pantai Depok, Bantul, Daerah Istimewa Yogyakarta]. *Seminar Nasional Kebumian ke-6.* (Yogyakarta: Teknik Geologi Universitas Gadjah Mada).

Giardino, A., Schrijvershof, R., Nederhoff, C. M., de Vroeg, H., Briere, C., Tonnon, P. K. and Caires, S., 2018, A Quantitative Assessment of Human Interventions and Clomate Change on the West African Sediment Budget. *Ocean and Coastal Management,* Vol. 156, 249-289.

Gracia, A., Rangel-Buitrago, N., Oakley, J. A. and Williams, A. T., 2018, Use of Ecosystems in Coastal Erosion Management. *Ocean and Coastal Management*, Vol. 156, 277-289.

Haryani, H., Irianto, A. and Nurhasan, S., 2019, Study of Coastal Abrasion Disasters and their Causes in Pariaman City. IOP Conference Series: Earth and Environmental Science, 1-11, DOI:10.1088/1755-1315/314/1/012009.

Hastie, T., Tibshirani, R. and Friedman, J., 2009, *The Element of Statistical Learning*, (New York: Springer).

Himmelstoss, E. A., Henderson, R. E., Kratzmann, M. G. and Farris, A. S., 2018, *Digital Shoreline Analysis System (DSAS) Verison 5.0 User Guide*. U.S. Geological Survey Open-File Report 2018-1179, 110.

Holloway, J., Helmstedt, K, J., Mengersen, K. and Schmidt, M., 2019, A Decision Tree Approach for Spatially Interpolating Missing Land Cover Data and Classifying Satellite Images. Remote Sensing, Vol. 11(15), 1796-1820.

Huete, A., Justice, C. and Leeuwen van, W. J. D., 1999, *MODIS Vegetation Index (MOD13) Algorithm Theoretical Basis Document*. USA.

Huete, A., Didan, K., Miura, T., Rodriguez, E. P., Gao, X. and Ferreira, L. G., 2002, Overview of the Radiometric and Biophysical Performance of the MODIS Vegetation Indices. *Remote Sensing of Environment*, Vol. 83(1-2), 195-213.

Indonesia Coordinating Minister of Maritime Affairs and Investment, 2018, *Indonesia Coordinating Minister of maritime Affairs and Investment Launches Reference Data on Indonesia Maritime Regions [Menko maritim Luncurkan Data Rujukan Wilayah Kelautan Indonesia]*. Accessed Juni 10, 2020. https://maritim.go.id/menko-maritim-luncurkan-data-rujukan-wilayah-kelautan-indonesia/.

Kandrika, S. and Roy, P. S., 2008, Land Use Land Cover Classification of Orissa Using Multi-Temporal IRS-P6 awifs Data: A Decision Tree Approach. *International Journal of Applied Earth Observation and Geoinformation*, Vol. 10(2), 186 – 193.

Louati, M., Saïdi, H. and Zargouni, F., 2014, Shoreline change Assessment Using Remote Sensing and GIS Techniques: A Case Study of the Medjerda Delta Coast, Tunisia. *Arabian Journal of Geosciences,* Vol. 8(6), 4239–4255.

Mahapatra, M., Ratheesh, R. and Rajawat, A. S., 2014, Shoreline Change Analysis along the Coast of South Gujarat, India, Using Digital Shoreline Analysis System. *Journal of the Indian Society of Remote Sensing,* Vol. 42(4), 869–876.

Malawani, M. N., Marfai, M. A., Hadmoko, D. S., Putra, M. D., Setiawan, N., Prakoso, S. H. and Mardiyanto, D., 2019, Shore Response Due to Tidal Wave Triggered by Cyclone in Daerah Istimewa Yoyakarta. *Majalah Ilmiah Globe*, Vol. 21 (2), 87-94.

Marfai, M. A., 2011, Impact of Coastal Inundation on Ecology and Agricultural Land Use Case Study in Central Java, Indonesia. *Questiones Geographicae*, Vol. 30(3), 19-32.

McFeeters, S. K., 1996, The use of the Normalized Difference Water Index (NDWI) in the Delineation of Open Water Features. *International Journal of Remote Sensing*, Vol. 17(7), 1425-1432.

Moore, L. J., 2000, Shoreline Mapping Techniques. *Journal of Coastal Research*, Vol. 16(1), 121-139.

Motohka, T., Nasahara, K. N., Oguma, H. and Tsuchida, S., 2010, Applicability of Green-Red Vegetation Index for Remote Sensing of Vegetation Phenology. *Remote Sensing*, Vol. 2(10), 2369-2387.

Mutaqin, B. W., 2017, Shoreline Changes Analysis in Kuwaru Coastal Area, Yogyakarta, Indonesia: An Application of the Digital Shoreline Analysis System (DSAS). *International Journal of Sustainable Development and Planning*, Vol. 12(7), 1203-1214.

Mutaqin, B. W., Agustina, N. and Permatasari, C. W., 2014, Characteristics of Waves in Kuwaru Waters during the East Monsoon. *Proceeding of 6th Indonesia Japan joint Scientific Symposium*. Yogyakarta.

Otsu, N., 1975, A Threshold Selection Method from Gray-Level Histograms. *Automatica*, Vol. 11, 23-27.

Otukei, J. R. and Blaschke, T., 2010, Land Cover Change Assessment Using Decision Trees, Support Vector Machines and Maximum Likelihood Classification Algorithms. *International Journal of Applied Earth Observation and Geoinformation*, Vol. 12(1), S27 – S31.

Pardo-Pascual, J. E., Almonacid-Caballer, J., Ruiz, L. A. and Palomar-Vazquez, J., 2012, Automatic Extraction of Shorelines from Landsat TM and ETM+ Multi-Temporal Images with Subpixel Precision. *Remote Sensing of Environment*, Vol. 123, 1-11.

PSBA, 2017, *Disaster Prone-Area Map Planning for jepara Regency [Penyusunan Peta Rawan Bencana Kabupaten Jepara].* (Yogyakarta: Pusat Studi Kebencanaan UGM).

Rais, J., Sulistyo, B., Diamar, S., Gunawan, T., Sumampouw, M., Soeprapto, T. A., Suhardi, I., Karsidi, A. and Widodo, M. S., 2004, *Arranging Integrated Marine Spaces [Menata Ruang Laut Terpadu]*. (Jakarta: PT Pradnya Paramita).

Rocha, A. V. and Shaver, G. R., 2011, Burn Severity Influences Postfire CO2 Exchange in Arctic Tundra. *Ecological Applications*, Vol. 21(2), 477-489.

Ryu, J. H., Won, J. S. and Min, K. D., 2002, Waterline Extraction from Landsat TM Data in a Tidal Flat: A Case Study in Gomso Bay, Korea. *Remote Sensing of Environment*, Vol. 83(3), 442-456.

Saputro, G. B., Marschiavelli, M. I. C., Ibrahim, F. and Edwin, M., 2017, Identification of Typology Related to the Coastal Line Changes in Bantul. *IOP Conference Series: Earth and Environmental Science*, 1-8.

Sinaga, T. P. T. and Susiati, H., 2007, Study of Shoreline Change Modeling of the Waters of the Muria Peninsula Studi Pemodelan Perubahan Garis Pantai di Sekitar Perairan Tapak PLTN Semenanjung Muria. *Jurnal Pengembangan Energi Nuklir*, Vol. 9(2).

Sunarto, 2004, *Geomorphic Changes of Coastal Area around Muria Volcano, Central Java: A Paleogeomorphological Study [Perubahan Fenomena Geomorfik Daerah Kepesisiran di Sekeliling Gunungapi Muria JawaTengah: Kajian Paleogeomorfologi]*. *Dissertation*, (Yogyakarta: Faculty of Geography, Universitas Gadjah Mada).

Thior, M., Sane, T., Dieye, E. B., Sy, O., Cissokho, D., Ba, B. D. and Descroix, L., 2019, Shoreline Dynamics of the Northern Lower Casamance (Senegal) and Southern Gambia Littoral from 1968 to 2017. *Journal of African Earth Sciences*, Vol. 160, DOI:10.1016/j.jafrearsci.2019.103611.

Torma, M., 2013, Land Cover Classification of Finnish Lapland Using Decision Tree Classification Algorithm. *The Photogrammetric Journal of Finland*, Vol. 23 (2).

Tourism Services of Bantul Regency, 2019, *Data on Tourism Object Visits [Data Kunjungan Objek Wisata 2019]*, (Bantul: Tourism Services of Bantul Regency).

Triatmodjo, B., 2008, *Beach Engineering [Teknik Pantai]*, (Yogyakarta: Beta Offset).

UNGEGN, 2019, *Country Report of The Republic of Indonesia*, (New York: UNGEGN).

van Westen, C. J., van Asch, Th. W. J. and Soeters, R., 2006, Landslide Hazard and Risk Zonation: Why is it Still So Difficult? *Bulletin of Engineering Geology and the Environment*, Vol. 65(2), 167-184.

Verhulp, J. and van Niekerk, A., 2017, Transferability of Decision Trees for Land Cover Classification in a Heterogeneous Area. *South African Journal of Geomatics*, Vol. 6(1), 30 – 46.

Vitousek, P. M., Mooney, H. A., Lubchenco, J. and Melillo, J. M., 1997, Human Domination of Earth's Ecosystems. *Science (Scienci)*, Vol. 277(5325), 494-499.

Wahidin, N., Siregar, V. P., Nababan, B., Jaya, I. and Wouthuyzen, S., 2015, Object-based Image Analysis for Coral Reef Benthic Habitat Mapping with Several Classification Algorithms. *Procedia Environmental Sciences*, Vol. 24, 222-227.

Wicaksono, A. and Wicaksono, P., 2019, Geomteric Accuracy Assessment for Shoreline Derived from NDWI, MNDWI and AWEI Transformation on Various Coastal Physical Ttypology in Jepara Regency usung Landsat 8 OLI Imagery in 2018. *Geoplanning: Journal of Geomatics and Planning,* Vol. 6(1), 55-72.

Wicaksono, A., Wicaksono, P., Khakhim, N., Farda, N. M. and Marfai, M. A., 2019, Semi-automatic Shoreline Extraction Using Water Index Transformation on Landsat 8 OLI Imagery in Jepara Regency. *Sixth International Symposium on LAPAN-IPB Satellite. Proc. SPIE 11372*.

Wicaksono, A. and Winastuti, R., 2020, Study of Coastal Morphodynamics and Abrasion Susceptibility in Buleleng Regency [Kajian Morfodinamika Pesisir dan Kerawanan Abrasi di Kabupaten Buleleng, Provinsi Bali]. *Prosiding Seminar Nasional Pengelolaan Pesisir dan Daerah Aliran Sungai ke-5. Tagerang Selatan*, 132-140.

Wicaksono, A., Khakhim, N., Pratama, D. N. D., Musthofa, A. and Lazuardi, W., 2021, Geometric Accuracy Comparison of Shorelines Derived from Multitemporal Sentinel-2a Imagery with Various Image Spectral Transformations (Case Study: Marine Deposition Coasts in Bantul Regency, Yogyakarta, Indonesia). *International Journal of geoinformatics,* Vol. 17(4), 27-40.

Xu, H., 2007, Modification of Normalised Difference Water Index (NDWI) to Enhance Open Water Features in Remotely Sensed Imagery. *International Journal of Remote Sensing*, Vol. 27(14), 3025-3033.